Proc. 14th Int. Conf. on Muon Spin Rotation, Relaxation and Resonance (μSR2017)
JPS Conf. Proc. **21**, 011052 (2018)
https://doi.org/10.7566/JPSCP.21.011052

Introduction and a quick look at MUESR, the Magnetic structure and mUon Embedding Site Refinement suite

Pietro Bonfà[1], Ifeanyi John Onuorah[2] and Roberto De Renzi[2]

[1]*CINECA, Casalecchio di Reno 6/3, 40033 Bologna, Italy*
[2]*Dipartimento di Scienze Matematiche, Fisiche e Informatiche, University of Parma, Parco delle Scienze 7A, 43124 Parma, Italy*

E-mail: p.bonfa@cineca.it

(Received June 25, 2017)

The estimation of the magnetic field generated at a given point by magnetic dipoles is an undergraduate exercise. However, under certain approximation, this is all that is needed to evaluate the local field at the muon site once the interstitial position of the muon in the unit cell is known. The development of an application to specifically solve this problem may therefore seem an excessive effort. At the same time, the lack of a general solution leads to the development of small *ad hoc* codes that are generally rewritten or re-adapted for different experiments and are poorly optimized. This and other motivations led to the development of MuESR, a python+C tool to perform dipolar field simulations. In this manuscript we will describe the tool, its features and its development strategies.

KEYWORDS: Muon spin rotation relaxation, Dipole fields, Muon sites

Introduction

With the advent of accurate and affordable electronic structure simulation methods, a new approach has emerged to solve the task of identifying the interstitial positive muon site in crystalline systems [1–8]. This information is particularly important for muon spin rotation and relaxation spectroscopy (μSR) experiments performed on magnetic materials since it allows to unveil quantitative information on the magnetic order under the study. Once the muon site is known, the evaluation of the local field at the muon site given a specific long range magnetic order is a trivial task. However one may be interested in evaluating the local field on a grid of muons sites or, like in the case of the Bayesian approach [9], on a large set of random interstitial points. Moreover, if the long range magnetic order is not known yet, one can possibly be interested in checking a set of allowed magnetic structures (obtained, for example, from representation theory or from maximal magnetic space groups) for a given propagation vector. And finally this test should be done considering all the crystallographically equivalent interstitial sites. This and other similar tasks make the trivial problem of evaluating the local field at the muon site quite time consuming, since, at the end of the day, the less time is dedicated to the development of a general purpose computer program by using ad hoc solutions, the more time will be required to adapt or rewrite the code for the future experiments. Moreover, this type of calculation is generally CPU bound and the development of sufficiently optimized codes can lead to spectacular algorithmic efficiencies. This however requires the use of more sophisticated coding strategies.

For this reason we started the development of a new program, called MuESR, for Magnetic structure and mUon Embedding Site Refinement, a Python based library with a self consistent C kernel that is responsible for the number crunching. The application has been designed and developed by μSR users for μSR users, thus keeping particular attention to some key points that will be discussed in the following sections: generality, efficiency and simplicity of use.

Implementation details

MuESR is a computer program written in the form of a C library and a python package that performs dipole-field and dipole-tensor sums using real space algorithms. While Ewald summation would provide an even more efficient method to perform the evaluation of the magnetic field generated by an infinite lattice of magnetic dipoles, its implementation is still missing in MuESR since the performances of modern laptops provide enough computational power to obtain results with better than 1% accuracy in generally less than a ms time per muon site. The time required to perform the simulations is therefore negligible on the scale of the full data analysis.

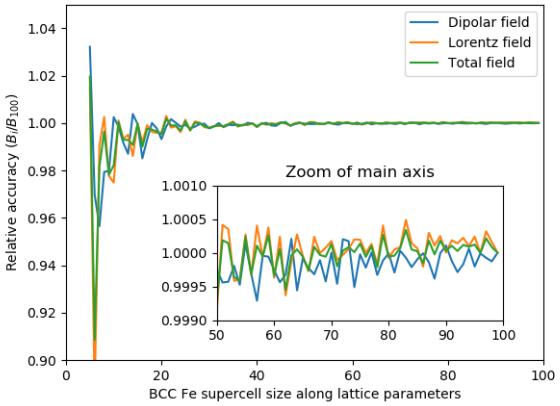

Fig. 1. Convergence against the supercell size for the components of Eq. 1 in the case of BCC Iron for the known muon site. The x axis reports the number of unit cells in the three lattice directions. The largest Lorentz sphere contained in the supercell is always considered.

The current implementation performs a dipolar field sum using the Lorentz method, which is briefly described in the following and is instead discussed in details, for example, in Ref. [10].

The total field at the muon site $\mathbf{B}_\mu$ in a zero-field experiment can be split for convenience in the following terms:

$$\mathbf{B}_\mu = \mathbf{B}_{\text{dip}} + \mathbf{B}_{\text{c}} + \mathbf{B}_{\text{dem}} \ , \tag{1}$$

where $\mathbf{B}_{\text{dip}}, \mathbf{B}_{\text{c}}$ and $\mathbf{B}_{\text{dem}}$ are the dipolar field, the Fermi contact field and the demagnetization field, respectively. In magnetic materials, the first two terms originates from the interaction between the muon and spin polarized electronic wavefunctions while the last term also depends on the sample geometry.

The dipolar field can be approximated with good accuracy, assuming a classical moment $\mathbf{m}$ centered at the atomic positions of the magnetic atoms, and evaluating the total contribution stemming from the electrons of the system as

$$\mathbf{B}_{\text{dip}}(\mathbf{r}) = \frac{\mu_0}{4\pi} \sum_i^N \left(\frac{3\mathbf{r_i}(\mathbf{m_i} \cdot \mathbf{r_i})}{r_i^5} - \frac{\mathbf{m_i}}{r_i^3} \right) \tag{2}$$

where $\mathbf{m}_i$ is the magnetic moment of atom i, $\mathbf{r}_i$ is the distance between atom i and the muon site and N is the total number of magnetic moments in the system under study.

To improve the convergence of this sum, the Lorentz method is generally adopted. In this approach, only the moments that reside inside a sphere of radius $\mathbf{R}_{\text{L}}$ from the muon position are ac-

tually summed as in Eq. 2, while the moments outside the so called Lorentz sphere are treated as a continuum. This last contribution is obtained, in MuESR, as

$$\mathbf{B}_{\mathrm{L}} = \frac{\mu_0}{3V_{\mathrm{L}}} \sum_{i}^{\mathbf{r}_i<\mathbf{R}_{\mathrm{L}}} \mathbf{m_i}(\mathbf{r_i}) \tag{3}$$

where V_L is the volume of the Lorentz sphere. In MuESR, the dipolar field is therefore reported as two separate components: $\mathbf{B}_{\mathrm{D}}$, stemming from the direct sum of the atoms inside the Lorentz sphere, and $\mathbf{B}_{\mathrm{L}}$.

The Fermi contact field contribution is instead of purely quantum origin. In MuESR, this term is evaluated assuming a scalar interaction between the muon and the spin polarized electron wavefunction ψ_s:

$$\mathbf{B}_{\mathrm{cont}} = \sum_{i}^{N_n} \frac{2\mu_0}{3} |\psi_s(\mathbf{r}_\mu)|^2 \mathbf{m}_i^s = \sum_{i}^{N_n} \frac{2\mu_0}{3} w_i A_c \mathbf{m}_i^s \tag{4}$$

where $\mathbf{r}_\mu$ is the muon position, N_n is a cut-off provided by a maximum distance from the muon, $w_i(\mathbf{r}_i, \mathbf{r}_\mu)$ is a scaling factor and A_c is a scalar coupling factor. There are two strong assumptions[1] in the above formula that are not guarantied to be valid in general. The first one is the assumption that the interaction is isotropic and can therefore be described with a scalar coupling term. The second one is the definition of the w_i term. In principle its value should be obtained from a quantum mechanical treatment of the electrons in the system. However, in lack of this sophisticate treatment, a possible approximation that can be introduced is to make it proportional to the distance r_i, i.e. the distance between the muon position and the atom having spin polarized orbitals. In the current implementation of MuESR this term is actually proportional to $1/r_i^3$. This setting can be modified, but requires the recompilation of the C source code. This is because, in the current classical approximation, a simple geometrical dependent description of this quantity is by definition arbitrary. Attention should be paid to this term to check if it matches the expected behavior since, especially in antiferromagnets, results can depend on the number of nearest neighbors N_n selected.

Finally, in MuESR the description of the magnetic structures is provided by means of the propagation vector formalism, requiring the definition of the magnetic moments in terms of Fourier components (FC), in a similar fashion to the FullProf [11], the neutron scattering analysis suite.

The general expression for the magnetic moment of a given atom j in the unit cell at $\mathbf{R}_l$ is

$$\mathbf{m}_{lj} = \sum_{\mathbf{k}} \mathbf{S}_{\mathbf{k}} \exp(-2\pi i(\mathbf{k}\mathbf{R}_l + \phi_{\mathbf{k}j})) \tag{5}$$

where $\mathbf{k}$ is the propagation vector, defined in reciprocal space, while $\mathbf{S}_{\mathbf{k}j}$ are the complex Fourier coefficients.

The vast majority of the magnetic orders can be described as the sum over just a few $\mathbf{k}$ wavevector components. At the time of writing, MuESR only implements single $\mathbf{k}$ orders, without real loss of generality, since the local field at the muon site generated by multiple $\mathbf{k}$ is just the sum of the local fields generated by each individual $\mathbf{k}$. This has the advantage of leaving the possibility of distinguishing the contributions given by the various $\mathbf{k}$ to the terms of Eq. 1.

The main reason for choosing the propagation vector formalism, instead of the alternative description in terms of magnetic space groups, is the possibility of using the representation analysis of magnetic structure as provided by the tools of the FullProf suite [11].

[1] Eq. 4 is actually obtained starting from the quantum Hamiltonian describing the interaction between an electron and a muon and using a series of approximations. The reader is referred to Ref. [10] for a detailed description of the origin and the validity of the above result.

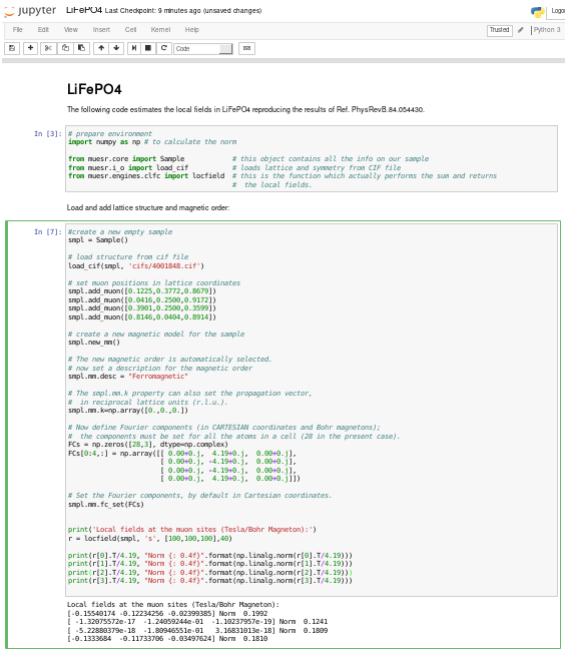

LiFePO4

The following code estimates the local fields in LiFePO4 reproducing the results of Ref. PhysRevB.84.054430.

In [3]:
```
# prepare environment
import numpy as np # to calculate the norm

from muesr.core import Sample           # this object contains all the info on our sample
from muesr.i_o import load_cif          # loads lattice and symmetry from CIF file
from muesr.engines.clfc import locfield # this is the function which actually performs the sun and returns
                                        #  the local fields.
```

Load and add lattice structure and magnetic order:

In [7]:
```
#create a new empty sample
smpl = Sample()

# load structure from cif file
load_cif(smpl, 'cifs/4001848.cif')

# set muon positions in lattice coordinates
smpl.add_muon([0.1225,0.3772,0.8679])
smpl.add_muon([0.0416,0.2500,0.9172])
smpl.add_muon([0.3901,0.2500,0.3599])
smpl.add_muon([0.8146,0.0404,0.8914])

# create a new magnetic model for the sample
smpl.new_mm()

# The new magnetic order is automatically selected.
# now set a description for the magnetic order
smpl.mm.desc = "Ferromagnetic"

# The smpl.mm.k property can also set the propagation vector,
#  in reciprocal lattice units (r.l.u.).
smpl.mm.k=np.array([0.,0.,0.])

# Now define Fourier components (in CARTESIAN coordinates and Bohr magnetons);
#  the components must be set for all the atoms in a cell (28 in the present case).
FCs = np.zeros([28,3], dtype=np.complex)
FCs[0:4,:] = np.array([[ 0.00+0.j,  4.19+0.j,  0.00+0.j],
                       [ 0.00+0.j, -4.19+0.j,  0.00+0.j],
                       [ 0.00+0.j, -4.19+0.j,  0.00+0.j],
                       [ 0.00+0.j,  4.19+0.j,  0.00+0.j]])

# Set the Fourier components, by default in Cartesian coordinates.
smpl.mm.fc_set(FCs)


print('Local fields at the muon sites (Tesla/Bohr Magneton):')
r = locfield(smpl, 's', [100,100,100],40)

print(r[0].T/4.19, "Norm {: 0.4f}".format(np.linalg.norm(r[0].T/4.19)))
print(r[1].T/4.19, "Norm {: 0.4f}".format(np.linalg.norm(r[1].T/4.19)))
print(r[2].T/4.19, "Norm {: 0.4f}".format(np.linalg.norm(r[2].T/4.19)))
print(r[3].T/4.19, "Norm {: 0.4f}".format(np.linalg.norm(r[3].T/4.19)))
```

```
Local fields at the muon sites (Tesla/Bohr Magneton):
[-0.15540174 -0.12234256 -0.02399385] Norm  0.1992
[ -1.32075572e-17  -1.24059244e-01  -1.10237957e-19] Norm  0.1241
[ -5.22880379e-18  -1.80946551e-01   3.16831013e-18] Norm  0.1809
[-0.1333684  -0.11733706 -0.03497624] Norm  0.1810
```

Fig. 2. The list of commands, in the form of a Python notebook, that are required to evaluate the local field in $LiFePO_4$ at the four muon sites proposed by Ref. [19]. Without comments, it's 25 lines of code (20 lines if print functions are neglected). Time to solutions is just a couple of seconds.

Description of the tool

The MuESR library is written in Python and C. It is compatible with both Python2 and Python3 and it can also be used in C or C++ programs, but in this latter case only the functions performing the dipole field sums and the dipolar tensor evaluation are available. The C code is self contained and has no dependencies, even if a computationally optimized set of routines (under development) will depend on external libraries. The python based part only depends on NumPy [12, 13], but some more packages are required to exploit all the functionalities provided by the code.

The simplest user experience can be obtained with interactive Python shells like IPython of Jupyter notebooks, as shown, for example, in Fig. 2. This approach also allows the production of simple and easily shareable documents and guarantees reproducible data.

The code itself is available on a GitHub repository (see Ref. [14]). A rather complete documentation, starting from installation instructions, including a tutorial and a number of guided examples, is available on the web [15]. The very simple examples include the case of an antiferromagnet, $LiFePO_4$, shown in Fig. 2, and a further example including the contact field is that of BCC Fe. As it may be seen, the python exploitation code reduces to twenty lines and produces its result on a standard personal computer in the order of a second.

The definition of a new crystalline structure, the starting point of all types of analyses, can be obtained by using the widespread functions provided by the ASE suite [16] (which has been slightly adapted in MuESR but preserve compatibility with the functions of the main project) or by loading CIF or XCrysDen [17] files. The code can use and collect symmetry information directly from the CIF files or using the Spglib [18] to inspect the symmetries starting from the lattice and atomic positions definition. This information can later be used to reduce the computational load or to explore all the possible symmetry equivalent sites of dipolar sum calculations. The core includes routines to obtain local fields as a function of the rotation of the local moments around a given axis and an optimized

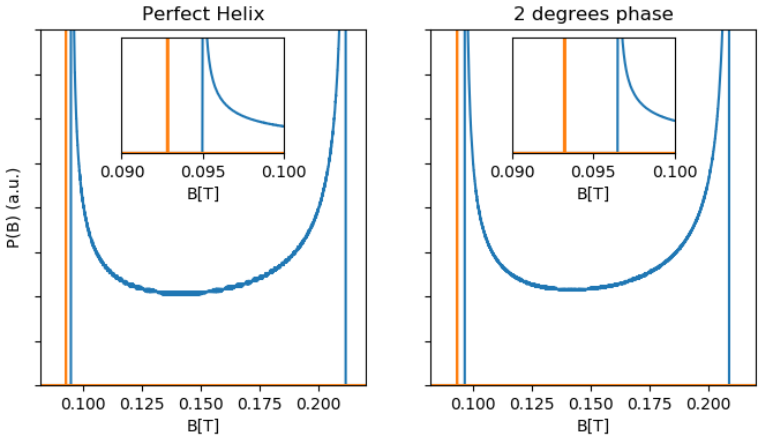

Fig. 3. Distribution of the local field at the muon sites in MnSi for a perfect left handed helical magnetic structure (right) and for the experimental magnetic structure described in Ref. [20] (left). For the sake of clarity, the single peak and the Overhauser distribution are depicted with different colors. The effect of a phase shift between the magnetic moments of the Mn inside the unit cell is evident from the zoomed inset panels.

algorithm for non-commensurate magnetic orders (see Ref. [4], appendix).

The current fully portable routines running on a single Core 2 Duo processor (2.5 GHz) require about 15 ms per muon site to achieve better than 2 parts per thousand accuracy. Nonetheless, since most of the time is spent in python function calls overhead in such a small case, the time to collect the results for 1000 sites with the same accuracy is just about 2.5 seconds [2].

Key studies

Let us now discuss the effectiveness of MuESR by introducing two representative studies. The first one is the interesting case of the helimagnet MnSi, which is also treated in the examples reported in Ref. [15].

There are four equivalent muon sites in the MnSi cell, made inequivalent by the choice of the direction of **k** in a single crystal [4, 21]. They give rise to a double peak spectrum, plus a sharp line shown in Fig. 3 [21]. It was pointed out by a recent experiment [20] that magnetic Mn ions are distinguished in orbits (in principle four, as many as the ions in the unit cell, experimentally only two), where the helix is realized by the same wave vector, but may be distinguished by a different relative phase. Neutron diffraction is insensitive to this detail, but μSR is not: the phase produces a relative shift between the double peak spectrum and the sharp line, shown in the insets of Fig. 3, that originate from the contribution of the four muon sites in the unit cell. It is very quick to reproduce this subtle difference with MuESR, as it is shown in the example reported in Ref. [15], thus determining the relative phase between the two orbits that reproduces the experimental result [20, 21].

Whenever the presence of a large contact field can be ruled out and the muon position is known, either from DFT simulations or from single crystal experiments, representation analysis for a given set of propagation vectors may be used to identify the long range magnetic order by comparing experimental and calculated dipolar fields at the muon sites.

Let's consider, as an example, $CuSe_2O_5$, a compound that has been thoroughly investigated in Ref. [22] with both μSR and Neutron scattering measurements. This material crystallizes in a mon-

[2] In addition, two experimental branches introduce OpenMP parallel execution that show very good scaling up to 4 cores and an interface to optimized BLAS functions which provide an order of magnitude better performances with respect to the trivial implementation, at the expenses of full code portability.

	Γ^1	Γ^3
x, y, z	(u, v, w)	(u, v, w)
$-x, y, -z + 1/2$	$(-u, v, w)$	$(u, -v, w)$

Table I. The combinations of Fourier amplitudes u, v, w in the irreducible representations of the little groups of $\mathbf{k} = (1, 0, 0)$ for $CuSe_2O_5$, which has a monoclinic cell with C2/c symmetry and Cu atoms in (0,0,0).

oclinic lattice structure [23] characterized by the presence of four magnetic Cu atoms per unit cell having a reduced moment of about half Bohr magneton. The lattice structure is depicted in Fig. 4 where the refined magnetic order is also represented.

From μSR data, the presence of four muon site can be guessed. The positions identified by Herak and co-workers are all close to oxygen atoms and are located in the $8f$ Wyckoff sites: (0.19,0.01,0.23), (0.33,0.40,0.06), (0.32,0.44,0.02) and (0.35,0.49,0.32). The dipolar magnetic fields at these sites are 19 mT, 31 mT, 32 mT and 54 mT respectively. These embedding positions were found with a dipolar field analysis described in detail in Ref. [22] but it will be assumed here that they are known from a transverse field experiment performed on a single crystal sample[3] or from a detailed DFT analysis[4].

From neutron scattering data analysis, the **k**=(1,0,0) propagation vector is identified and the little group of the propagation vector can be decomposed into two irreducible representations reported in the header of Tab. I. The values for the local moments of the Cu atoms can therefore be expressed as a linear combination of the FC factors as reported in Tab. I. This reduces the number of degrees of freedom in the definition of the magnetic order from 6 to 3, thus making it fairly easy to explore this phase space with the constraint of a fixed absolute value for the local moment per Cu atom.

After 10000 uniform random samples of the u, v and w parameters varying on a sphere, a set of compatible magnetic moment directions, belonging to Γ^3, can reproduce the absolute value of the experimental magnetic fields at the muon sites (with better than 5 mT accuracy on each site) while no compatible configurations are found for Γ_1 under the same conditions. This result agrees well with the neutron scattering magnetic refinement discussed in Ref. [22] which reports that the best agreement with the experimental data is obtained with Γ^3.

The local moment directions on the Cu atoms obtained from the u, v and w parameters exploration are shown in Figure 4b. With the given threshold of 5 mT for the comparison with the modulus of the experimental fields, two set of vectors are obtained and one of them share the same direction of the Cu moments provided by the Rietveld refinement, although with lower accuracy. This is partially due to the fact that the propagation vector is at the border of the Brillouin zone thus making the norm of local field at the muon sites the same for all the equivalent positions in the unit cell. Nonetheless, it is possible to rule out the irreducible representation Γ^1 and to confirm that Cu moments almost lie in the $b - c$ plane. The use of MuESR makes this result readily obtainable.

Conclusions

The MuESR tool presented in this article represents a simple but complete and optimized method to evaluate the local field at the muon site. It can be used from within a scripting language thus providing enough flexibility to the user and to allow the implementation of a variety of approaches for the muon embedding site identification and/or for long range magnetic order investigations.

The tool is opensource, documented and freely available under GPLv3.

[3] A single crystal sample is actually available for this compound.

[4] The authors of Ref [22] tried to identify the muon site by inspecting the minima of the unperturbed electrostatic potential. This approach is however inaccurate in insulators as they point out.

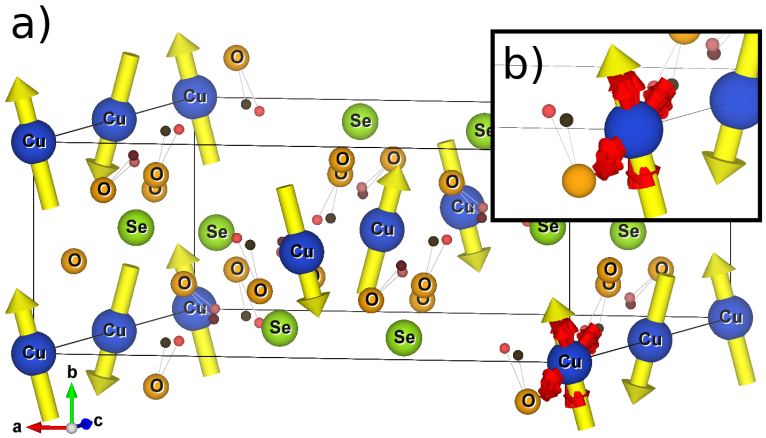

Fig. 4. Results of the dipolar field based investigation of the magnetic order of $CuSe_2O_5$. The atoms of the hosting system have labels reporting the element name while the (coloured) dots with grey thin links show the muon sites and their distance from Oxygen atoms. The yellow (long) arrows show the zero field long range magnetic order, obtained with neutron scattering magnetic refinement, which belongs to the irreducible representation Γ^3. The smaller red arrows, also shown in the zoomed panel b), indicate the compatible magnetic orders (see main text) obtained by varying the u, v and w parameters. Only 10% of the full set is shown. This subset share the same characteristics of the whole set of the compatible parameters, i.e. the local moments on Cu atoms have small a component and two definite values for the c component. The direction of the moments on the other Cu atoms is not reproduced for the sake of clarity since it is fixed by symmetry. Produced with VESTA [24].

Acknowledgemnts

We thank Anthony Lim, Matteo Aramini and Stephen Cottrell for trying, debugging and discussing the code development. This work is funded by the European Union's Horizon 2020 research and innovation programme under grant agreement No 654000.

References

[1] F. R. Foronda, F. Lang, J. S. Möller, T. Lancaster, A. T. Boothroyd, F. L. Pratt, S. R. Giblin, D. Prabhakaran, and S. J. Blundell. *Phys. Rev. Lett.* **114**, 017602, Jan (2015).
[2] J. S. Möller, D. Ceresoli, T. Lancaster, N. Marzari, and S.J. Blundell. *Phys. Rev. B* **87**, 121108(R) (2013).
[3] C. G. Van de Walle. *Phys. Rev. Lett.* **64**, 669 (1990).
[4] N. Martin, M. Deutsch, F. Bert, D. Andreica, A. Amato, P. Bonfà, R. De Renzi, U. K. Rößler, P. Bonville, L. N. Fomicheva, A. V. Tsvyashchencko, and I. Mirebeau. *Phys. Rev. B* **93**, 174405 (2016).
[5] P. Bonfà, F. Sartori, and R. De Renzi. *J. Phys. Chem. C* **119(8)**, 4278–4285 (2015).
[6] F. Bernardini, P. Bonfà, S. Massidda, and R. De Renzi. *Phys. Rev. B* **87**, 115148 (2013).
[7] J. S. Möller, P. Bonfà, D. Ceresoli, F. Bernardini, S. J. Blundell, T. Lancaster, R. De Renzi, N. Marzari, I. Watanabe, and S. Sulaiman. *Physica Scripta* **88** (2013).
[8] G. Prando, P. Bonfà, G. Profeta, R. Khasanov, F. Bernardini, M. Mazzani, E. M. Brüning, A. Pal, V. P. S. Awana, H.-J. Grafe, B. Büchner, R. De Renzi, P. Carretta, and S. Sanna. *Phys. Rev. B* **87**, 064401 (2013).
[9] S. J. Blundell, A. J. Steele, T. Lancaster, J. D. Wright, and F. L. Pratt. *Physics Procedia* **30**, 113 – 116 (2012). 12th International Conference on Muon Spin Rotation, Relaxation and Resonance (μSR2011).
[10] A. Yaouanc and P. Dalmas de Réotier. *Muon Spin Rotation Relaxation and Resonance: Applications to Condensed Matter*. Oxford University Press, Oxford, (2011).
[11] J. Rodriguez-Carvajal. Fullprof: a program for rietveld refinement and pattern matching analysis. In *satellite meeting on powder diffraction of the XV congress of the IUCr*, volume 127. Toulouse, France], (1990).

[12] P. F. Dubois, K. Hinsen, and J. Hugunin. *Computers in Physics* **10**, May/June (1996).
[13] D. Ascher, P. F. Dubois, K. Hinsen, J. Hugunin, and T. Oliphant. *Numerical Python*. Lawrence Livermore National Laboratory, Livermore, CA, ucrl-ma-128569 edition, (1999).
[14] P. Bonfà, I. J. Onuorah, and R. De Renzi. MuESR. `http://www.github.com/bonfus/muesr`, (2017). [Online; accessed 19-June-2017].
[15] P. Bonfà, I. John Onuorah, and R. De Renzi. MuESR Docs. `http://muesr.readthedocs.io`, (2017). [Online; accessed 19-June-2017].
[16] A. H. Larsen, J. J. Mortensen, J. Blomqvist, I. E. Castelli, R. Christensen, M. Dułak, J. Friis, M. N. Groves, B. Hammer, C. Hargus, E. D. Hermes, P. C. Jennings, P. B. Jensen, J. Kermode, J. R. Kitchin, E. L. Kolsbjerg, J. Kubal, K. Kaasbjerg, S. Lysgaard, J. B. Maronsson, T. Maxson, T. Olsen, L. Pastewka, A. Peterson, C. Rostgaard, J. Schiøtz, O. Schütt, M. Strange, K. S. Thygesen, T. Vegge, L. Vilhelmsen, M. Walter, Z. Zeng, and K. W. Jacobsen. *Journal of Physics: Condensed Matter* **29**, 273002 (2017).
[17] A. Kokalj. *Computational Materials Science* **28**, 155 – 168 (2003). Proceedings of the Symposium on Software Development for Process and Materials Design.
[18] A. Togo. Spglib. `https://atztogo.github.io/spglib/`, (2017). [Online; accessed 19-June-2017].
[19] J. Sugiyama, H. Nozaki, M. Harada, K. Kamazawa, O. Ofer, M. Månsson, J. H. Brewer, E. J. Ansaldo, K. H. Chow, Y. Ikedo, Y. Miyake, K. Ohishi, I. Watanabe, G. Kobayashi, and R. Kanno. *Phys. Rev. B* **84**, 054430, Aug (2011).
[20] P. Dalmas de Réotier, A. Maisuradze, A. Yaouanc, B. Roessli, A. Amato, D. Andreica, and G. Lapertot. *Phys. Rev. B* **95**, 180403, May (2017).
[21] A. Amato, P. Dalmas de Réotier, D. Andreica, A. Yaouanc, A. Suter, G. Lapertot, I. M. Pop, E. Morenzoni, P. Bonfà, F. Bernardini, and R. De Renzi. *Phys. Rev. B* **89**, 184425, May (2014).
[22] M. Herak, A. Zorko, M. Pregelj, O. Zaharko, G. Posnjak, Z. Jagličić, A. Potočnik, H. Luetkens, J. van Tol, A. Ozarowski, H. Berger, and D. Arčon. *Phys. Rev. B* **87**, 104413, Mar (2013).
[23] R. Becker and H. Berger. *Acta Crystallogr. Sect. A* **62**, i256–i257, Dec (2006).
[24] K. Momma and F. Izumi. *J. Appl. Cryst.* **41**, 653–658, 06 (2008).